International Journal of Pharmacy and Pharmaceutical Sciences

ISSN- 0975-1491 Vol 8, Issue 7, 2016

Original Article

FLOURIDE REMOVAL FROM SEWAGE WATER USING *CITRUS LIMETTA* PEEL AS BIOSORBENT

TEJ PRATAP SINGH[1], C. B. MAJUMDER[2*]

Department of Chemical Engineering, IIT Roorkee, Roorkee 47667, Uttarakhand, India
Email: cbmajumder@gmail.com

Received: 22 Jan 2016 Revised and Accepted: 17 May 2016

ABSTRACT

Objective: The aim of this paper is to study the fluoride removal efficiency of the *citrus limetta* peel as low-cost biosorbent for defluoridation of sewage waste water.

Methods: For finding the best operating condition for maximum removal of fluoride, batch wise experiments were performed at different contact times and keeping other parameters to be constant such as pH, initial fluoride concentration, and adsorbent dose. Various kinetic models such as intraparticle diffusion model, Bangham's model, Elovich model had been investigated for determining the suitable adsorption mechanism. The rate of adsorption of fluoride on *citrus limetta* peel has been determined by pseudo first-order and pseudo second order rate models. SEM analysis has been used for describing the surface morphology of the peel. The surface characterization of the *citrus limetta* peel has been investigated by using the FTIR and EDAX analysis.

Results: The adsorption kinetics rate and the mechanism were best described by the pseudo-second order model and Bangham's model, respectively. The optimum pH, initial concentration, adsorbent dose and contact time were found to be 7, 20 mg/l, 10 g/l and 40 min. respectively for which there was maximum fluoride removal.

Conclusion: The result obtained from the experiments show that the *citrus limetta* peel has proved to be a low-cost biosorbent for the defluoridation of the sewage waste water and has high fluoride removal efficiency.

Keywords: Batchwise Biosorption Experiment, Bangham's Model, Langmuir Isotherm, SEM analysis, FTIR analysis

INTRODUCTION

Fluoride contamination is one of the major health problems all around the world. Generally, the effluents released from various industries cause the increase in fluoride level in ground water which tends to be toxic to both aquatic and terrestrial life. When the level of fluoride in drinking water is above a certain limit, it causes dental and skeletal fluorosis in human beings [1, 2]. The permissible limit of fluoride concentration in drinking water has been set as 1.5 mg/l by various environmental regulatory authorities like WHO and USEPA etc. A report published by Rajiv Gandhi National Drinking Water Mission in 1983 identified 15 states including Delhi as endemic for fluorosis. Table 1 depicts states which are presently, endemic for fluorosis [3].

Table 1: Information on the occurrence of excessive fluoride in ground water in India

State	No. of habitation with excess fluoride	State	No. of habitation with excess fluoride
Andhra Pradesh	7548	Madhya Pradesh	201
Gujarat	2378	Orissa	1138
Karnataka	860	Punjab	700
Kerala	287	Rajasthan	16560
Meghalaya	33	Tamil Nadu	527
Haryana	334	Uttar Pradesh	1072
Himachal Pradesh	488	West Bengal	21

Generally, contamination of fluoride in water is of natural origin which is dissolved in water from the fluoride deposits (rocks like topaz, cryolite and fluorapatite, etc.) on earth [4]. Further, various industries such as electroplating, glass, ceramics, steel manufacturing and phosphate fertilizer production, etc. also cause contamination of fluoride in ground water. Due to the scarce resources of drinking water, there is a need of treatment of contaminated water so it can be further used. At present, various techniques are used for the treatment of waste water such as ion exchange, coagulation, electro dialysis, dialysis, Nano filtration and reverse osmosis, etc [5-18]. All these processes have high operating cost due to which bio-sorbents are getting more attention nowadays due to their abundant availability and low cost. Different kinds of literature are available on the removal of fluoride from water using bio-sorbents like neem leaf, rice husk ash, peepal leaf, mosambi peel, banana peel, khair leaf, etc [19-22]. In this paper, the fluoride removal potential of *citrus limetta* peel has been investigated for the removal of fluoride from water.

MATERIALS AND METHODS

Citrus limetta peel was collected from a fruit stall located in the campus of IIT Roorkee Uttarakhand, India. After collection, the peel was washed, dried and crushed for the preparation of bio-sorbent and then screened through the 350 µm mesh. All chemicals used in the batch study were purchased from Fisher Scientific, LobaChemie and were of analytical grade. Stock solution (100 mg/l) of fluoride was prepared from distilled water by dissolving 221 mg anhydrous sodium fluoride in one-liter water [23].

Batch bio-sorption experiment

To conduct a batch experiment on fluoride removal is known the quantity of bio-sorbent (10 g/l) was added in a conical flask of volume 100 ml containing synthetic waste water sample (50 ml) of 20 mg/l initial fluoride concentration which was followed by shaking at 120 rpm [19,20]. Ranges of operating parameters for the experiment are shown in table 2.

Table 2: Ranges of operating parameters for contact time experiment

Objective of experiment	Operating parameters
To study the effect of time on fluoride removal	Adsorbent Dose: 10 g/l; Initial Fluoride Concentration: 20 mg/l; Room Temperature: 30 °C; Solution pH: 7;Contact Time: 5, 10, 15, 20, 25, 30, 45, 60 min

In the experiment, the solution was filtered through Whatman no. 42 filter paper after adsorption [30] and the filtrate was analyzed through SPADNS photometric method, at 570 nm using the UV–spectrophotometer (UV–210 A, SHIMADZU, Australia) to determine fluoride concentration. The fluoride concentration retained in the adsorbent phase, q_e (mg/g), was calculated according to the following formula-

$$q_e = (C_i - C_f) \times \frac{V}{W}$$

Where, q_e is the amount of fluoride adsorbed (mg/g)

C_i is the initial concentration of fluoride at equilibrium (mg/l)

C_f is the residual concentration of fluoride at equilibrium (mg/l)

W is the weight (g) of the adsorbent

V is the volume (l) of the solution.

The % absorption (A) of fluoride was calculated as follows

$$\% \text{ Adsorption} = \frac{(C_i - C_f)}{C_i} \times 100$$

Experimental data on the removal of fluoride from water generated through the variation of time were used to regress model kinetic equations and compute the kinetic parameters, whereas, the equilibrium models were regressed with the data generated through the variation of initial fluoride concentration and isotherm constants were computed.

Spectrophotometric methods

In this method, the metallic compound such as aluminium, iron, thorium, zirconium, lanthanum or cerium reacts with an indicator dye to build a complex having small dissociation constant. This complex reacts with fluoride to form a new complex. Because of the transformation in the complex configuration, the surface assimilation spectrum also shifts relative to the spectrum for the fluoride-free reagent solutions. This alteration can be observed by using a spectrophotometer.

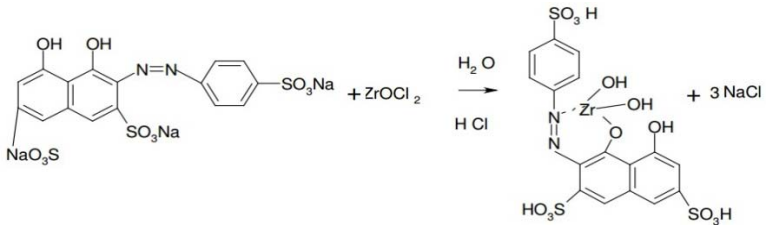

Formation of the SPADNS–ZrOCl2 complex

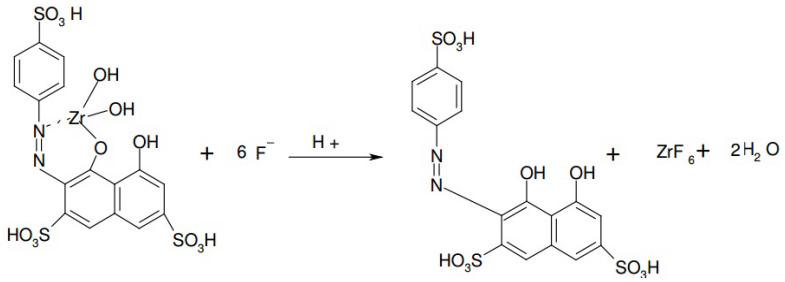

Reaction of the complex with fluoride ions

Recipe for SPADNS Solution

$$\frac{\text{Mg of Fluoride}}{\text{Litre}} = \frac{A}{\text{Sample (ml)}} \times \frac{B}{C}$$

Where

A represents Fluoride obtained by Curve (mg)

B represents diluted sample final volume (ml)

C represents diluted sample volume worn for the development of color.

$$\frac{\text{Mg of Fluoride}}{\text{Litre}} = \frac{A_0 - A_x}{A_0 - A_1}$$

Where

A_0 represents Absorbance at Zero Fluoride Concentration

A_1 represents Absorbance at Fluoride Concentration of 1 mg/l

A_x represents Absorbance of sample prepared

RESULTS AND DISCUSSION

Effect of contact time

The effect of contact time on the removal efficiency of the *citrus limetta* was explained by a plot between time t (min) and the amount of fluoride absorbed q_t (mg/g) as shown in Fig.1. The removal of fluoride increases initially with an increase in agitation time. But after the contact time of 40 min, it gradually tends to a constant value, denoting the equilibrium state due to the saturation of the active sites of the biosorbent.

A similar trend was also observed by other scholars during adsorption of fluoride onto *citrus limetta* peel [24]. With respect to contact time, *citrus limetta* peel reached saturation after 40 min, which was fixed as their optimum contact time. After the 40 min. the deviation in the fluoride removal efficiency is very small i.e. almost negligible.

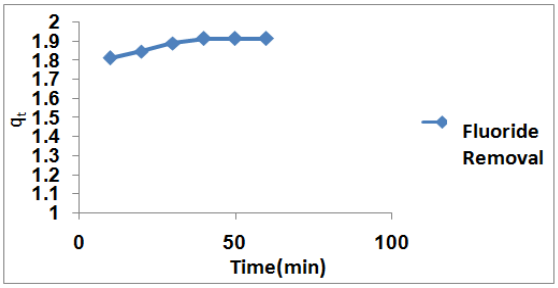

Fig. 1: Effect of contact time on adsorption of fluoride on *citrus limetta* peel

Adsorption kinetics

The adsorption kinetics of the fluoride removal by *citrus limetta* was explained by using various kinetics models such as pseudo first-order, pseudo second-order, Weber and Morris intra-particle diffusion model, Elovich equation and Bangham's pore diffusion model.

The best fitted kinetic model was found by the squared sum of errors (SSE) values. It is assumed that the model which gives the lowest SSE values is the best model for the particular system [25, 26]. The SSE values were calculated using the equation,

$$SSE = \sum (qe_{expt} - qe_{cal})^2 / (qe_{expt})^2$$

Where

$q_{e\ (expt)}$ is the experimental sorption capacity of fluoride (mg/g) at equilibrium

$q_{e\ (cal)}$ is the calculated sorption capacity of fluoride (mg/g) at equilibrium

The SSE values and various kinetic parameters for all the kinetic models were calculated and mentioned in table 3.

Pseudo first order model

The Lagergren's rate equation has been widely used for describing the rate equation for the adsorption of adsorbate from the liquid phase [27]. The linearized form of the pseudo first-order rate expression is given as:

$$log(q_e - q_t) = log(q_e) - \frac{k_1 t}{2.303}$$

Where

q_e is the amount of fluoride adsorbed on adsorbent (mg/g)

q_t is the amount of fluoride adsorbed on adsorbent at equilibrium and at time t (min)

k_1 is the rate constant of pseudo-first-order kinetics

Fig. 2 shows the plot which is the linearized form of a pseudo-first-order kinetic model for the *citrus limetta* peel bio-sorbent.

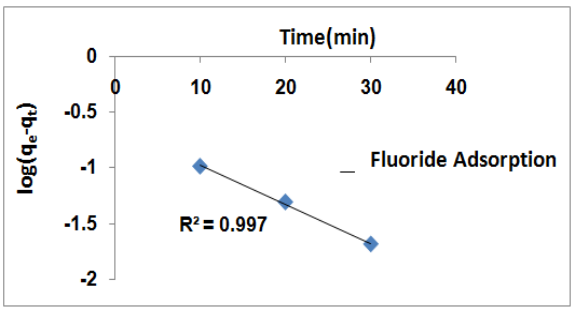

Fig. 2: Pseudo first order kinetic modeling of adsorption of fluoride onto *Citrus limetta* Peel

The plots were found to be linear with good correlation coefficients (>0.9) indicating the applicability of pseudo-first-order model in the present study. The values of the pseudo first-order rate constant (k_1) and $q_{e(cal.)}$ were determined for the adsorbent from the slope and the intercept of corresponding plot and are listed in table 3.

Pseudo-second order model

The adsorption kinetics can also describe as pseudo-second order process using the following equation [28],

$$\frac{t}{q_t} = \frac{1}{q_e^2 . k_2} + \frac{1}{q_e}$$

Where,

q_e and q_t have the same meaning as mentioned previously and k_2 is the rate constant for the pseudo-second-order kinetics. The plots of t/q_t versus t for the adsorbents are shown in fig. 3. The values of $q_{e\ (cal.)}$ and k_2 were determined for each adsorbent from the slope and intercept of the corresponding plot and are compiled in table 3.

The correlation coefficient (R2) values for pseudo-second-order adsorption model have high values, i.e. 0.999 for the bio-adsorbent *citrus limetta* peel. The R2 value is higher than that of pseudo-first-order model. The lower SSE values for pseudo second order model also indicate that the adsorption kinetics of fluoride onto *citrus limetta* peel can be better described by pseudo-second-order model. A similar phenomenon has observed by others for the adsorption of fluoride on many adsorbents [29, 30].

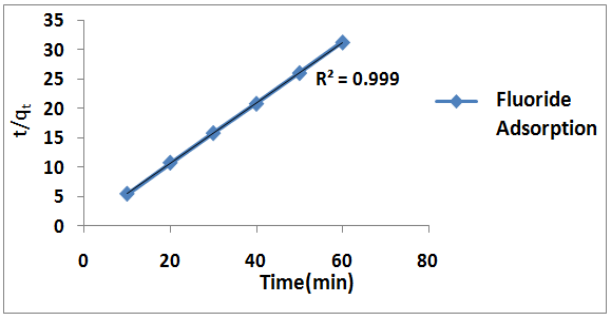

Fig. 3: Pseudo second order kinetic modeling of adsorption of fluoride onto *Citrus limetta* peel

Intra-particle diffusion

Rate of sorption is frequently used to analyze nature of the 'rate-controlling step' and the use of the intra-particle diffusion model has been greatly explored in this regard which is represented by the following Weber and Morris equation [31]–

$$q_t = k_{ip} \times t^{0.5} + C$$

Where,

C_i-the intercept, determined by the thickness of the boundary layer.

Kip-the intra-particle diffusion rate constant.

According to this model, if adsorption of a solute is controlled by the intra-particle diffusion process, a plot of q_t versus $t^{1/2}$gives a straight line. Weber and Morris plots of q_t versus $t^{\circ.5}$are shown in fig. 4 for citrus limetta peel. It is evident from the plots that the reared two separate stages; first linear portion (Stage I) and second curved path followed by a plateau (Stage II). In Stage I, nearly 50% of fluoride was rapidly taken up by bio-sorbent within 5 min. This is attributed to the immediate utilization of the most readily available adsorbing sites on the adsorbent surfaces. In Stage II, very slow diffusion of adsorbate from the surface site into the inner pores is observed. Thus, the initial portion of fluoride adsorption by carbon adsorbents may be governed by the initial intraparticle transport of fluoride controlled by a surface diffusion process, and later part is controlled by pore diffusion. Similar dual nature with initially linear and then plateau was also found in some literature [32]. Though intra-particle

diffusion renders straight lines with correlation coefficient more than 0.98 for the *citrus limetta* bio-sorbent and the intercept of the line fails to pass through the origin in each case. This can be explained by the difference in the rate of mass transfer in the initial and final stages of adsorption [33] and indicates some degree of boundary layer control which implies that intra-particle diffusion is not only rate controlling step [27]. The data were further used to learn about the slow step occurring in the present adsorption system using pore diffusion model.

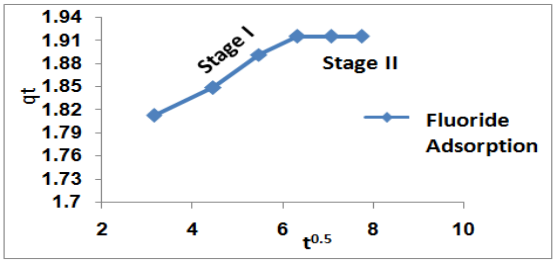

Fig. 4: Intra-particle diffusion plot *citrus limetta* peel

Bingham's model

Bangham's model for adsorption process is described by Bingham's model equation [33].

$$\log\log\left(\frac{C_i}{C_i - q_t.m}\right) = \log\left(\frac{K_0.m}{2.303.V}\right) + \alpha.\log(t)$$

Where

C_i-The initial concentration of the adsorbate in a solution (mg/l)

V - Volume of solution in (ml)

m - Mass of the adsorbent (g/l)

q_t - The amount of adsorbate retained at time t (mg/g)

K_0 - Constant

$$\log\log\left(\frac{C_i}{C_i - q_t.m}\right)$$

To plot versus log t (fig. 4) for *citrus limetta* peel. The plot was found to be linear for adsorbent with correlation coefficient indicating that kinetics confirmed Bangham's equation and therefore the adsorption of fluoride onto *citrus limetta* peel, was pore diffusion controlled. A similar trend was observed in the literature for the adsorption of fluoride onto waste carbon slurry [34].

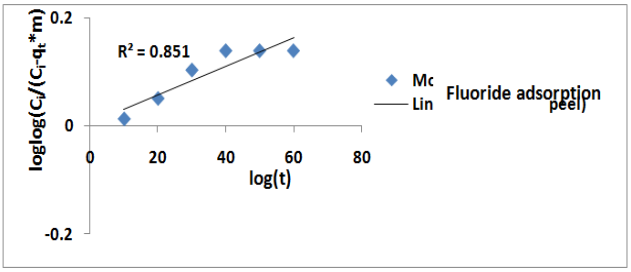

Fig. 5: Bangham's model pore diffusion plot of *citrus limetta* peel

Elovich equation

The Elovich equation [35]:

$$q_t = \frac{ln(\alpha\beta t)}{\beta} + \frac{ln(t)}{\beta}$$

Where,

α - Initial sorption rate (mg/g min)

β - Extent of surface coverage and activation energy for chemisorptions

When q_t versus ln (t) is plotted on a sheet of the graph as shown in fig. 6, the result follows Elovich equation. Confirmation to this equation alone might be taken as evidence that the rate determining step is diffusion in nature [36]. And this equation should apply at conditions where desorption rate can be ignored [37]. The kinetic curve of sorption demonstrated good fitting with the model (R^2>0.9) which may indicate the diffusion rate-limiting is more prominent in fluoride sorption by *citrus limetta* peel. The similar results are also found in previous literature [38].

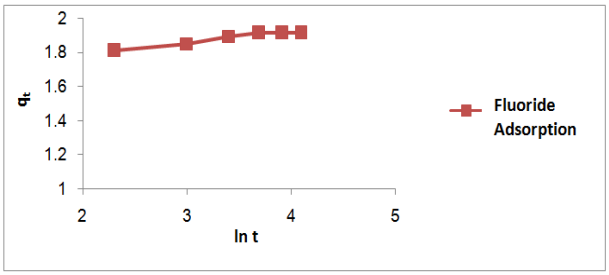

Fig. 6: Elovich equation plots for *Citrus Limetta* peel

Table 3: Pseudo first-order, pseudo second order, Weber and Morris, Bangham's and Elovich model's parameters and calculated $q_{e(cal)}$ and experimental $q_{e(expt)}$ values at 20 mg/l fluoride concentrations for all five kinetics models stated above

Pseudo first order						
Name of adsorbent	k_1 (1/min)	$q_{e(expt)}$(mg/g)		$q_{e(cal)}$(mg/g)	R^2	SSE
citrus limetta peel	0.392	1.92		0.33	0.9978	0.68
Pseudo-second order						
Name of adsorbent	k_2 (1/min)	$q_{e(expt)}$(mg/g)		$q_{e(cal)}$(mg/g)	R^2	SSE
citrus limetta peel	0.679	1.92		1.91	0.9999	0.0001
Intra-particle diffusion model						
Name of adsorbent	k_{ip} (mg/g$\sqrt{min}$)	$q_{e(expt)}$(mg/g)		$q_{e(cal)}$(mg/g)	R^2	SSE
citrus limetta peel	0.0265	1.92		1.73	0.9366	0.0096
Bangham's model						
Name of adsorbent	k_0	$q_{e(expt)}$(mg/g)	$q_{e(cal)}$(mg/g)	R^2	α	SSE
citrus limetta peel	11.61	1.92	1.81	0.8651	0.019	0.0032
Elovich equation						
Name of adsorbent	B	$q_{e(expt)}$ (mg/g)	$q_{e(cal)}$(mg/g)	R^2	α	SSE
citrus limetta peel	15.91	1.92	0.48	0.9671	0.061	0.566

Nomenclature: α is Initial sorption rate (mg/g. min)., β is related to extent of surface coverage and activation energy for chemi-sorptions, k_1 is the rate constant of pseudo-first-order kinetics, k_2 is the rate constant for the pseudo-second-order kinetics, q_e is the amount of fluoride adsorbed on adsorbent (mg/g), q_t is the amounts of fluoride adsorbed on adsorbent at equilibrium and at time t (min)., Kip is the intra-particle diffusion rate constant, $R^2$is the correlation coefficient, SSE is sum of squared error.

Characterization of biosorbent

SEM analysis

The surface morphology of the *citrus limetta* peel was demonstrated by SEM analysis as shown in fig. 7(a) and (b), which shows the scanning electron micrograph (SEM) of *citrus limetta* peel before and after adsorption studies respectively. SEM analysis shows that adsorbent had porous and irregular surface.

This analysis states that the surface porosity is mainly responsible for the adsorption.

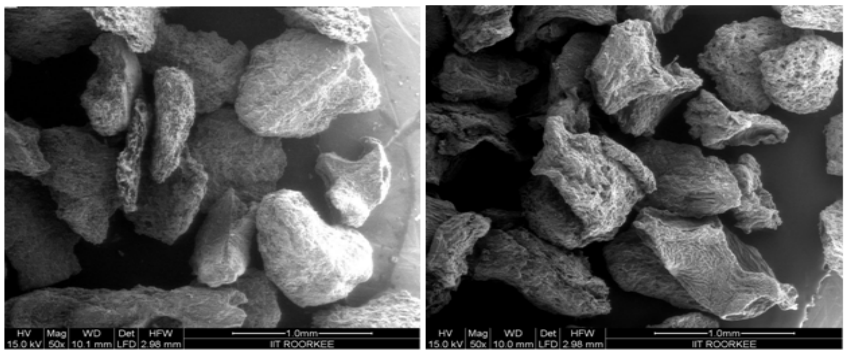

Fig. 7: SEM Micrograph of *citrus limetta* peel (a) Before bio-sorption process (b) After bio-sorption process

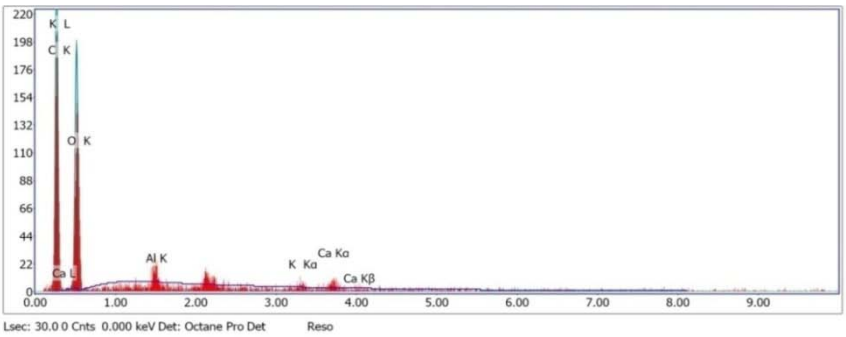

(a)

eZAF Smart quant results				
Element	**Weight %**	**Atomic %**	**Net Int.**	**Error %**
C K	45.23	53.28	55.4	7.89
O K	51.07	45.16	55.46	11.31
AlK	1.43	0.75	5.43	36.15
K K	0.58	0.21	1.36	67.85
CaK	1.69	0.6	3.22	61.77

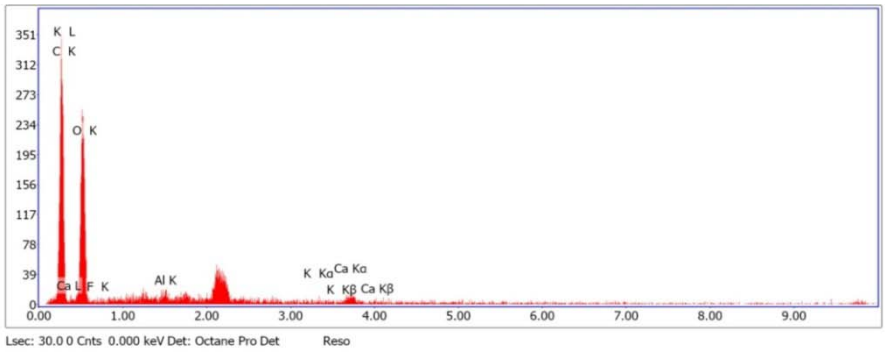

(b)

eZAF smart quant results				
Element	**Weight %**	**Atomic %**	**Net Int.**	**Error %**
C K	44.49	52.41	90.43	7.12
O K	51.93	45.93	92.44	10.67
F K	0.78	0.58	1.06	82.63
AlK	0.47	0.25	2.86	66.31
K K	0.29	0.11	1.1	69.29
CaK	2.04	0.72	6.25	31.12

Fig. 8: EDAX analysis of *citrus limetta* peel (a) Before bio-sorption process (b) After bio-sorption

EDAX analysis

The EDAX analysis of *citrus limetta* peel before and after adsorption Fluoride is shown in fig. 8(a) and 8(b). It is evident that various elements such as oxygen, carbon and very small amount of calcium were present initially but the fluoride was not present before adsorption. When the EDAX analysis was carried out after the fluoride adsorption, it was found that 0.78 % by wt of the fluoride was present which confirmed the bio-sorption of fluoride.

FTIR analysis

Functional groups present in bio-sorbents before and after adsorption of fluoride was determined by using Fourier transform infrared spectroscopy (Thermo Nicolet, Magna 7600). The samples were prepared by the pellet (pressed disk) method by mixing the same amount of KBr in each sample. Fig. 9(a) and 9(b) shows FTIR spectra on *citrus limetta* biosorbent in the selected spectral range of 4000-400 cm, which gives evident about the presence of many functional groups on the surface of the biosorbent.

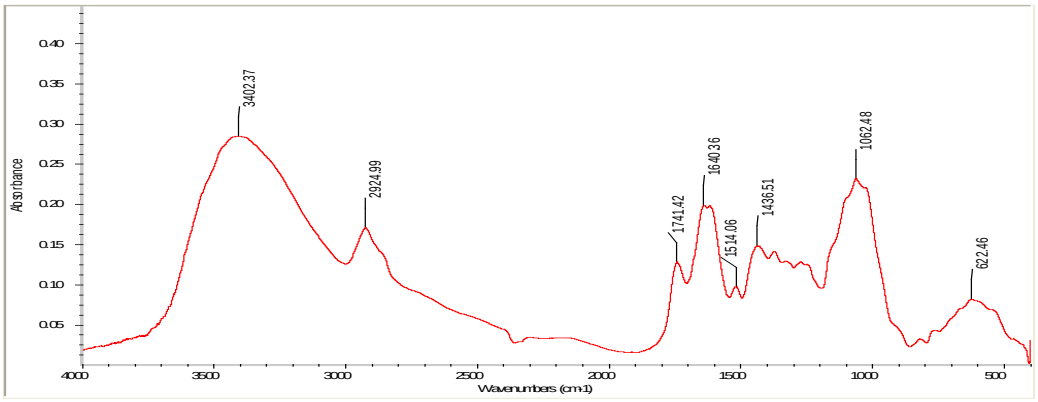

Fig. 9(a): Pictorial Representation of FTIR of *citrus limetta* peel before adsorption

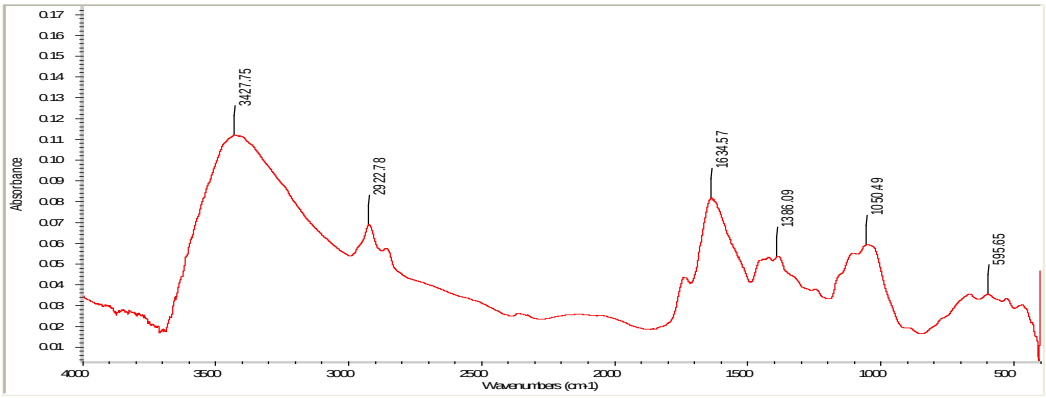

Fig. 9(b): Pictorial Representation of FTIR of *citrus limetta* peel after adsorption

Table 4: FTIR analysis for adsorbent in tabular form

Wave number (1/cm)	Compound	Groups
3200-3600	Alcohol	O-H
2500-3300	Carboxylic Acids & Derivatives	COO-H (very Broad)
1550-1650	Amines	NH_2 Scissoring (1 ° amines)
1350-1480	Alkane	-C-H
970-1250	Alcohols & Phenols	C-O
500-600	Alkyl Halide	C-Br
1620-1680	Alkene	C=C
675-1000	Alkene	=C-H
3500-3700	Alcohol	O-H

The ranges of different wave numbers are assigned to different functional groups present in the adsorbent. The alcohol is seen in the range of 3200-3600 and 3500-3700 while alcohol with the presence of phenol can be found out in the IR range of 970-1250. On the similar basis, alkenes are found in three IR ranges namely 1350-1480, 1620-1680 and 675-1000.

Alkyl Halide with IR range of 500-600 is also seen with Amines at 1550-1650. Carboxylic Acids & Derivatives were also observed at 2500-3300.

CONCLUSION

This investigation demonstrated the economic feasibility of the *citrus limetta* peel in bio-sorption of fluoride. During the study, it was found that the adsorption kinetics was best described by pseudo-second order model which explains the chemisorption rate of the adsorption. Though the plot of intra-particle diffusion was found to be a straight line with a high correlation coefficient close to 1 but the plot did not pass through the origin. This suggests that the adsorption kinetics was complex in nature with more than one

sorption mechanism. The kinetics was best fitted with the Bangham's model which states that rate limiting step of the adsorption was pore diffusion controlled. The characterization of the surface by SEM analysis reveals that adsorbent surface is porous and irregular, and this porosity is only responsible for the fluoride adsorption. EDAX analysis confirmed that fluoride is absorbed through citrus limetta peel and FTIR analysis described the presence of various functional groups on the adsorbent's surface. All these investigations show that the *citrus limetta* peel can be efficiently used for the fluoride removal.

CONFLICT OF INTERESTS

Declared none

REFERENCES

1. Bell MC, Ludwig TG. The supply of fluoride to man: ingestion from water, fluorides, and human health. WHO Monograph series 59. WHO, Geneva; 1970.
2. Singh R, Maheshwari RC. Defluoridation of drinking water: a review. Indian J Environ Prot 2001;21:983-91.
3. Malay DK, Salim AJ. Comparative study of batch adsorption of fluoride using commercial and natural adsorbent. Res J Chem Sci 2011;1:68-75.
4. Heck WW, Brandt CS. Effects on vegetation: native, crops, forests. Air Pollut 1977;2:157-229.
5. Maheshwari RC. Fluoride in drinking water and its removal. J Hazard Mater 2006;137:456-63.
6. Tor A, Danaoglu N, Arslan G, Cengeloglu Y. Removal of fluoride from water by using granular red mud: batch and column studies. J Hazard Mater 2009;164:271-8.
7. Popat KM, Anand PS, Dasare BD. Selective removal of fluoride ions from water by the aluminium form of the aminomethyl phosphonic acid-type ion exchanger. React Polym 1994;23:23-32.
8. Meenakshi S, Viswanathan N. Identification of selective ion-exchange resin for fluoride sorption. J Colloid Interface Sci 2007;308:438-50.
9. Haron MJ, Wan Yunus WMZ. Removal of fluoride ion from aqueous solution by a cerium-poly (hydroxamic acid) resin complex. J Environ Sci Health 2001;A36:727-34.
10. Sundaram CS, Viswanathan N, Meenakshi S. Defluoridation chemistry of synthetic hydroxyapatite at nanoscale: equilibrium and kinetic studies. J Hazard Mater 2008;155:206-15.
11. Sundaram CS, Viswanathan N, Meenakshi S. Uptake of fluoride by nano-hydroxyapatite/chitosan, a bioinorganic composite. Bioresour Technol 2008;99:8226-30.
12. Chubar NI. Adsorption of fluoride, chloride, bromide, and bromate ions on a novel ion exchanger. J Colloid Interface Sci 2005;291:67-74.
13. Kabay N, Arar Ö, Samatya S, Yüksel Ü, Yüksel M. Separation of fluoride from aqueous solution by electrodialysis: effect of process parameters and other ionic species. J Hazard Mater 2008;153:107-13.
14. Sujana MG, Thakur RS, Das SN, Rao SB. Defluorination of waste waters. Asian J Chem 1997;9:561-70.
15. Hichour M, Persin F, Sandeaux J, Gavach C. Fluoride removal from waters by Donnan dialysis. Sep Purif Technol 1999;18:1-11.
16. Matsuura T, Sourirajan S. Studies on reverse osmosis for water pollution control. Water Res 1972;6:1073-86.
17. Simons R. Trace element removal from ash dam waters by nanofiltration and diffusion dialysis. Desalin 1993;89:325-41.
18. Guo, Laodong, Becky JH, Peter HS. Ultrafiltration behavior of major ions (Na, Ca, Mg, F, Cl, and SO 4) in natural waters. Water Res 2001;35:1500-8.
19. Mondal NK, Bhaumik R, Banerjee A, Datta JK, Baur T. A comparative study on the batch performance of fluoride adsorption by activated silica gel and activated rice husk ash. Int J Environ Sci 2012;2:1643-61.
20. Pandey DD, Tripathi A, Singh TP. Removal of flouride from industrial waste water using mosambi peel as biosorbent: kinetics studies. Int J Sci Eng Technol 2016;4:304-13.
21. Jamode AV, Sapkal VS, Jamode VS. Defluoridation of water using inexpensive adsorbents. J Indian Inst Sci 2013;84:163.
22. Singh TP, Majumder CB. Removal of fluoride using treated banana peel in the batch reactor: kinetics and equilibrium studies. World J Pharm Pharm Sci 2015;4:693-704.
23. American Public Health Association. Standard methods for the examination of water and wastewater. Am Public Health Assoc 1915;2.
24. Singh TP, Majumder CB. Removal of fluoride using sweet lemon peel in the batch reactor: kinetics and equilibrium studies. World J Pharm Pharm Sci 2015;4:775-87.
25. Bayari CS, Kazanci N, Koyuncu I, Ağıralioğlu N, Gökçe D. Determination of the origin of the waters of Köyceğiz Lake, Turkey. J Hydrol 1995;166:171-91.
26. Viswanathan N, Sundaram CS, Meenakshi S. Removal of fluoride from aqueous solution using protonated chitosan beads. J Hazard Mater 2009;161:423-30.
27. Meenakshi S, Viswanathan N. Identification of selective ion-exchange resin for fluoride sorption. J Colloid Interface Sci 2007;308:438-50.
28. Lagergren S. About the theory of so-called adsorption of soluble substances; 1898. p. 1-39.
29. Weber WJ, Morris JC. Preliminary appraisal of advanced waste treatment processes. Proc Int Conf Advances Water Poll Res 1963;2:231-41.
30. Simons R. Trace element removal from ash dam waters by nanofiltration and diffusion dialysis. Desalin 1993;89:325-41.
31. Liao XP, Shi BI. Adsorption of fluoride on zirconium (IV)-impregnated collagen fiber. Environ Sci Technol 2005;39:4628-32.
32. Kumar E. Defluoridation from aqueous solutions by granular ferric hydroxide (GFH). Water Res 2009;43:490-8.
33. Aharoni, Chaim, Sideman S, Hoffer E. Adsorption of phosphate ions by collodion-coated alumina. J Chem Technol Biotechnol 1979;29:404-12.
34. Gupta VK, Ali I, Saini VK. Defluoridation of wastewaters using waste carbon slurry. Water Res 2007;41:3307-16.
35. Aharoni C, Ungarish M. Kinetics of activated chemisorption. Part 2.—Theoretical models. J Chem Soc Faraday Trans 1977;73:456-64.
36. Pavlatou A, Polyzopolus NA. The role of diffusion in the kinetics of phosphate desorption: the relevance of the Elovich equation. J Soil Sci 1988;39:425-36.
37. Rudzinksi W, Panczyk P, Schwarz JA, Contescu CI. Surfaces of nanoparticles and porous materials, Dekker, New York; 1998. p. 355.
38. Singh TP, Majumder CB. Kinetics for removal of fluoride from aqueous solution through adsorption from mousambi peel, groundnut shell and neem leaves. Int J Sci Eng Technol 2015;3:879-83.